*Canadian Mineralogist*
Vol. 31, pp. 61-73 (1993)

# PLATINUM-GROUP MINERALS FROM THE SANTIAGO RIVER, ESMERALDAS PROVINCE, ECUADOR

THOROLF WEISER AND MICHAEL SCHMIDT-THOMÉ

*Federal Institute for Geosciences and Natural Resources (BGR), P.O. Box 51 01 53, D-3000 Hannover 51, Germany*

## ABSTRACT

The first platinum-group minerals (PGM) to be described in detail from Ecuador come from placers in the Santiago River, Esmeraldas Province. This area is situated between the Cordillera de Toisán and the Pacific coast in the northwestern part of the country. The only PGM found as individual mineral grains in the placers are Pt–Fe alloys, mainly native platinum with minor isoferroplatinum. Minerals found as inclusions in Pt–Fe alloys are hongshiite, osmium, bowieite, cuprorhodsite, laurite, erlichmanite, cooperite, braggite, unknown phases in the systems Pd–As–Te, Pd–Cu–S and Pt–Cu–S, and chalcopyrite. The PGM in the placers are inferred to derive from a mafic–ultramafic Alaskan-type intrusion that has yet to be identified.

*Keywords*: platinum-group minerals, placer deposits, Pt–Fe alloys, Ru–Os–Ir alloy, PGE sulfides, Alaskan-type intrusion, Esmeraldas Province, Ecuador.

## SOMMAIRE

Nous décrivons ici pour la première fois les minéraux du groupe du platine des graviers alluvionnaires de la rivière Santiago, province d'Esmeraldas (Équateur). La région est située entre la Cordillère de Toisán et la côte du Pacifique, dans le nord-ouest du pays. Les seuls minéraux du groupe du platine dans ces graviers font partie d'alliages Pt–Fe; il s'agit surtout de platine natif, avec isoferroplatine accessoire. On trouve, en inclusions dans ces alliages, hongshiïte, osmium, bowieïte, cuprorhodsite, laurite, erlichmanite, cooperite, braggite, des phases méconnues des systèmes Pd–As–Te, Pd–Cu–S et Pt–Cu–S, et chalcopyrite. Un massif mafique–ultramafique de type Alaska, que nous n'avons pas encore identifié, serait à l'origine de ces pépites.

(Traduit par la Rédaction)

*Mots-clés*: minéraux du groupe du platine, alliages Pt–Fe, alliage Ru–Os–Ir, sulfures des éléments du groupe du platine, complexe intrusif de type Alaska, province d'Esmeraldas, Équateur.

## INTRODUCTION

The area between the Cordillera de Toisán and the Pacific coast in Esmeraldas Province, northwestern Ecuador, particularly between the rivers Cayapas, San Miguel, and Santiago, is well known for its occurrences of platinum-group minerals (PGM) and gold placers. In 1967, we carried out a geological investigation in this area. Attempts to collect platinum grains by panning stream and terrace sediments along the Santiago River failed; only a few grains of gold were recovered. However, the Compañia Minera Gowanda S.A., which holds a mining license along the banks of the Santiago River near the village of Playa de Oro, kindly provided several grains of platinum-group minerals from that area for our scientific investigation. This paper provides the first detailed account of the composition and origin of platinum-group minerals from the Ecuadorian Western Cordillera.

## GEOLOGY

A summary of the geology of the study area is given below. This summary is mainly based on the findings of Baldock (1982, 1985), Evans & Whittaker (1982), Henderson (1981), Kennerly (1980), Paladines & Sanmartin (1980), and on unpublished technical reports kindly provided by the Ecuadorian Geological Survey, the Instituto Ecuadoriano de Minería (INEMIN).

Ecuador is divided into three very distinct physiographic belts, the Costa, the Sierra, and the Oriente. All trend approximately NNE–SSW and also show differences in their geological and tectonic evolution (Fig. 1). The eastern part of the study area belongs to the Sierra belt, and the western part, to the Costa belt.

### *The Sierra*

The Cordillera de Toisán forms part of the Western

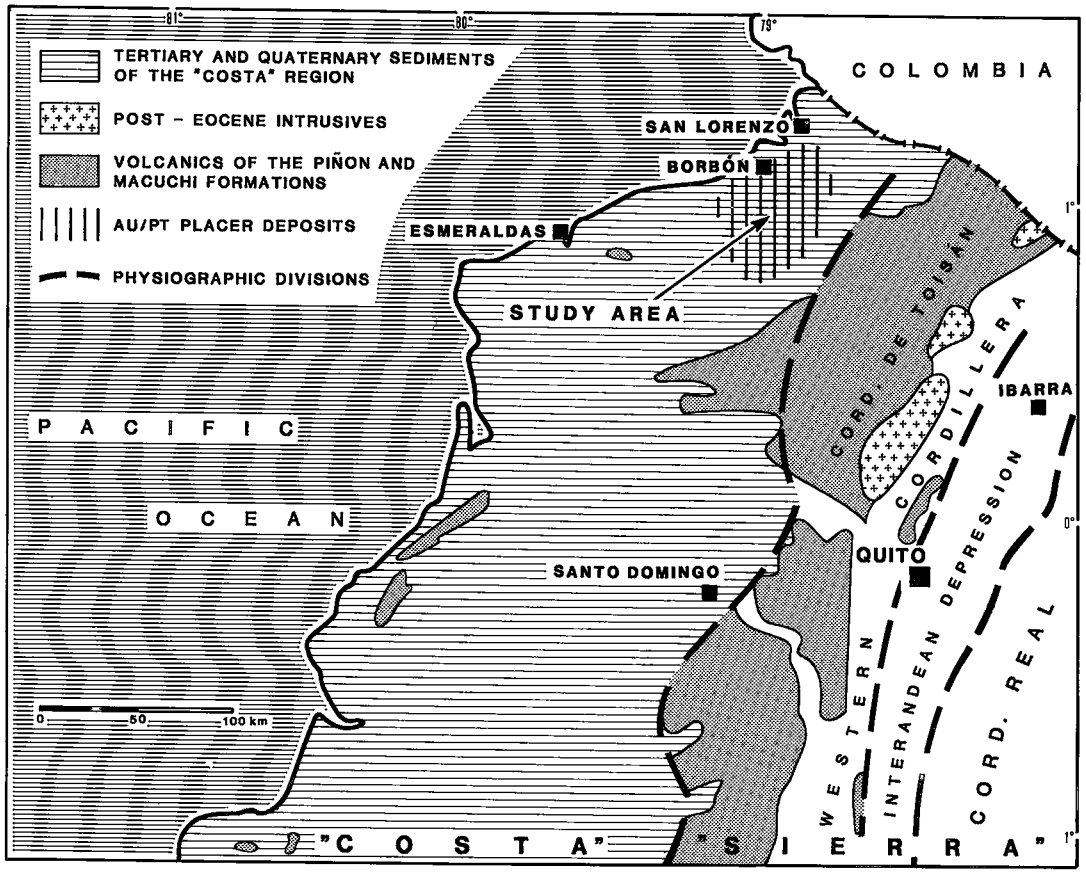


FIG. 1. Geological map of northwestern Ecuador (modified after Henderson 1981).

Cordillera (Cordillera Occidental) of Ecuador. Its western flank is mainly composed of intermediate volcanic rocks of the Macuchi Formation, which is of Late Cretaceous (Turonian–Coniacian) to Eocene age. This formation belongs to a volcanic-arc assemblage and has a probable thickness in excess of 8,000 m. Sequences within this formation where non-volcanogenic sediments are more common have been designated as the Chontal Member.

Andesitic volcanic rocks referred to as the San Juan de Lachas Volcanic Complex also occur on the western slopes of the Cordillera de Toisán. The age relation of these rocks to the Macuchi Formation are unclear, as the contacts are faulted.

Several plutonic bodies intrude the Macuchi Formation. They form the Apuela Batholith, for which a post-Eocene age is suspected. The batholith varies in composition from granite to diorite. Basic to ultrabasic dyke-like bodies (gabbros and gabbronorites) rarely occur within the Macuchi Formation. They have been interpreted as part of an ophiolite body that is considered to be the source rock of the PGM placers in the rivers west of the Cordillera de Toisán.

Late Eocene to early Oligocene orogenic movements also have affected the Macuchi Formation. Strong folding on a N–S axis and block faulting have occurred, but are rarely evident owing to the generally homogeneous nature of the volcanic complex.

*The Costa*

The Piñon Formation consists of basaltic lavas and breccias of submarine origin in which pillow structures are common. They may represent oceanic crust. Neither the extent nor the thickness of the Piñon Formation is known. Its age is pre-Senonian; it is older than the Macuchi Formation and may underlie part of it.

To the west, the volcanic complexes of the Macuchi

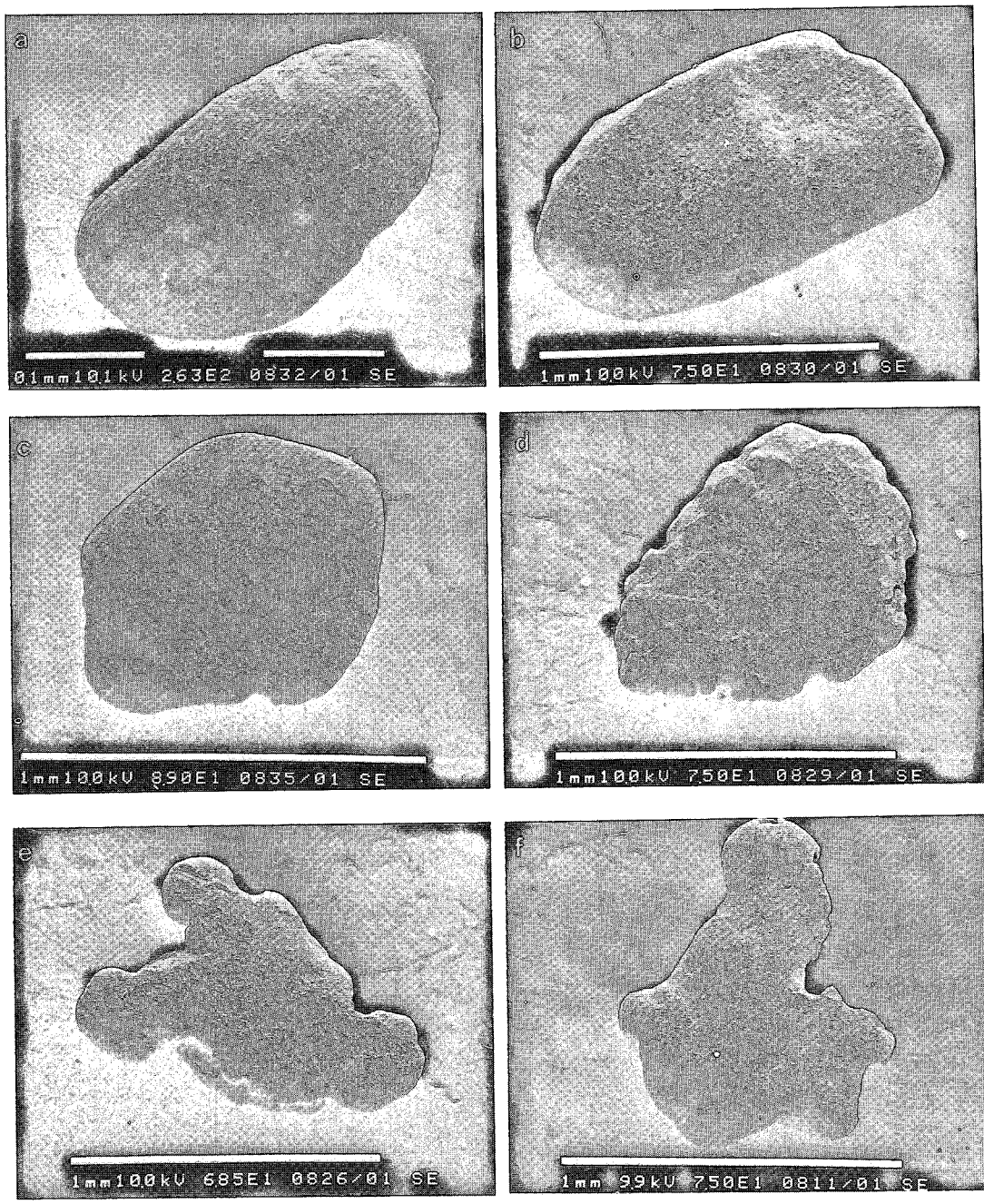


FIG. 2. SEM photomicrographs of typical grains of Pt–Fe alloy from the Santiago River. a, b. Smooth rounded elongate grains. c, d. Tabular grains with partly preserved primary crystal face(s). e, f. Tabular grains with lobed outlines.

and Piñon formations are overlain by Tertiary to Quaternary sedimentary sequences. They reach a maximum thickness of several thousand meters in the Borbón Basin. The sequences are typical of those in an idealized residual forearc basin and show alternation of shallow- and deep-water sedimentation caused by regional tectonic events. They are folded into a series of open NE–SW folds with sinuous traces. The faults mostly trend NNW–SSE; some of them run parallel to the coastline. All are normal faults; there is no evidence of thrusting.

The youngest deposits are more or less compacted fluviatile and estuarine sediments of Quaternary age derived from erosion of the Sierra to the east. The placer deposits of PGM and gold occur in these sediments and form an economic base, albeit a local one, for this region.

TABLE 1. CHEMICAL COMPOSITION* OF Pt-Fe AND Pt-Cu ALLOYS

| Analysis | 22 | 26 | 69 | 71 | 95 | 99 | 146 |
|---|---|---|---|---|---|---|---|
| | | | weight per cent | | | | |
| Ru | – | 0.25 | 0.28 | 0.31 | – | 0.12 | – |
| Rh | 1.33 | 1.39 | 1.52 | 1.16 | 0.83 | 2.36 | – |
| Pd | 3.45 | – | 0.19 | 0.81 | 0.66 | 0.20 | – |
| Os | 0.36 | 0.66 | 2.23 | 0.88 | 0.87 | 0.55 | 0.26 |
| Ir | 0.28 | 0.56 | 11.03 | 1.35 | 1.62 | 3.45 | 0.23 |
| Pt | 86.28 | 91.09 | 79.83 | 88.50 | 85.76 | 87.11 | 73.69 |
| Fe | 6.32 | 5.10 | 5.05 | 5.35 | 8.57 | 5.40 | – |
| Cu | 0.69 | 0.31 | 0.54 | 0.79 | 0.50 | 0.36 | 25.27 |
| Total | 98.71 | 99.36 | 100.67 | 99.33 | 98.81 | 99.55 | 99.45 |
| | | | atomic proportions | | | | |
| Ru | – | 0.004 | 0.005 | 0.005 | – | 0.002 | – |
| Rh | 0.021 | 0.023 | 0.025 | 0.019 | 0.013 | 0.039 | – |
| Pd | 0.053 | – | 0.003 | 0.013 | 0.010 | 0.003 | – |
| Os | 0.003 | 0.006 | 0.020 | 0.008 | 0.007 | 0.005 | 0.002 |
| Ir | 0.002 | 0.005 | 0.096 | 0.012 | 0.013 | 0.030 | 0.002 |
| Pt | 0.719 | 0.798 | 0.686 | 0.758 | 0.700 | 0.749 | 0.485 |
| Fe | 0.184 | 0.156 | 0.151 | 0.165 | 0.244 | 0.162 | – |
| Cu | 0.018 | 0.008 | 0.014 | 0.021 | 0.013 | 0.010 | 0.511 |

* Obtained by electron-microprobe analysis. All other elements were found to be below their limits of detection.

## Sample Preparation and Microprobe Techniques

For optical examination and electron-microprobe analyses, part of the heavy-mineral concentrate and the PGM were mounted in araldite and polished with diamond powder on a Dürener polisher with lead laps. A total of 103 individual grains of PGM were analyzed. The electron-microprobe analyses were carried out with a CAMEBAX Microbeam instrument using wavelength-dispersion spectrometry. The operating voltage was 20 kV at a beam current of 30 nA and a measurement time of 10 s. The following X-ray lines and standards were used: Ru$L\alpha$, Rh$L\alpha$, Os$M\alpha$, Ir$L\alpha$, Au$L\alpha$, Ag$L\beta$, Cu$K\alpha$, Ni$K\alpha$ (metals), Pt$K\alpha$, and Fe$K\alpha$ (synthetic $Pt_3Fe$ alloy), Pd$L\alpha$ (synthetic PdS), S$K\alpha$ (pyrite), Te$L\alpha$ (synthetic $Pd_3HgTe$), As$L\alpha$ (synthetic GaAs) and Sb$L\alpha$

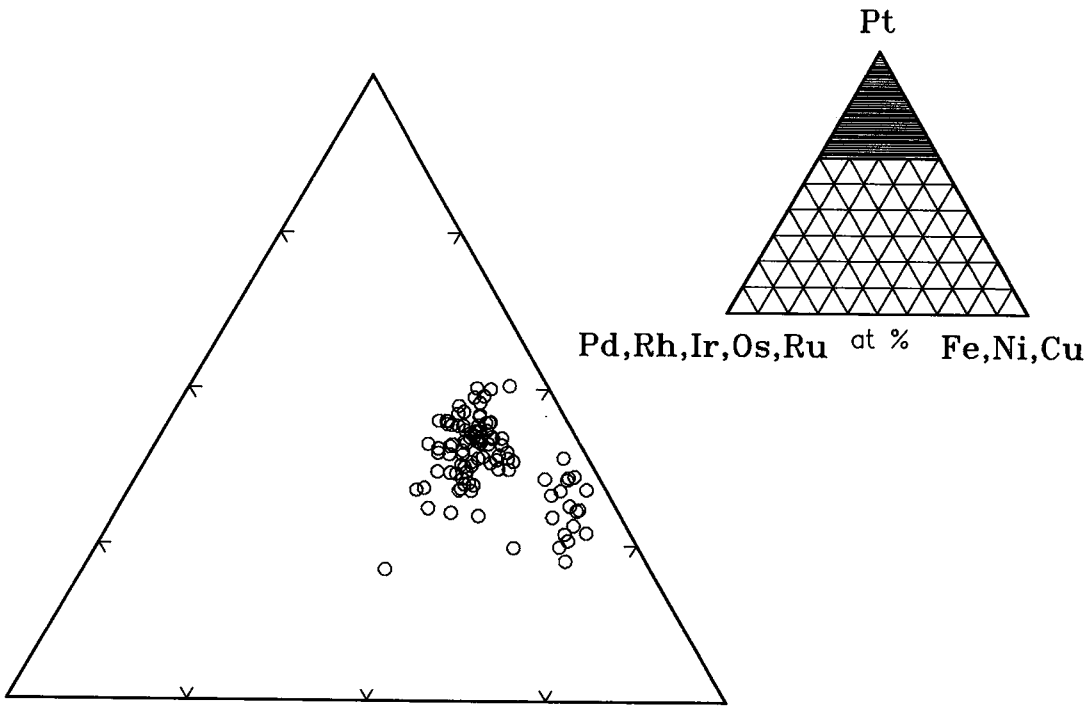


FIG. 3. Plot of bulk compositions (electron-microprobe data) of the Pt–Fe alloys.

(stibnite). Raw data were corrected using the PAP correction program (CAMECA), and correction of peak overlap was carried out for the elements Rh, Pd, Ag, Cu, As, and Sb. Altogether, 164 quantitative analyses were made on single grains and inclusions of PGM and native gold.

## Mineralogy

The heavy-mineral fraction mainly consists of ilmenite, which forms euhedral to subhedral crystals up to 500 μm in diameter. Under the microscope, the ilmenite may show lamellae of hematite and drop-like inclusions of pyrrhotite and chalcopyrite. Chromite is not very common in the concentrate; euhedral grains measure up to 500 μm across and show alteration at their margin. The grains of gold, which also are not very common, are flattened and have a lobed outline. Their size varies between 200 μm and 1 mm. Microprobe analyses gave an average content of 8.2 wt.% Ag; no other elements could be detected. The only platinum-group mineral (PGM) found as discrete grains are Pt–Fe alloys. All other observed PGM occur only as inclusions in Pt–Fe alloys and rarely as a replacement along grain margins.

### *Pt–Fe alloys*

The single grains are between 100 μm and 1.5 mm in size. They are mostly rounded (Figs. 2a, b) or flattened with lobed outlines (Figs. 2e, f). In some cases, a primary crystal face is partly preserved (Fig. 2c). Microprobe analyses show that all grains examined, apart from the fact that they contain inclusions, are homogeneous. The Pt content varies from grain to grain, mainly between 70 and 80 at.% (Table 1, Fig. 3). Only three grains have a Pt content greater than 80 at.%. The elements Ru, Rh, Pd, Os, Ir, and Cu are present in all grains, whereas Ni is absent. The grains contain between 1 and 15 at.% Ru + Rh + Pd + Os + Ir, and about 80% of the compositions fall in the range 4 – 8 at.%. A conspicuous feature is the consistently very low content of Ru, which never reaches more than 0.5 wt.%, showing good accordance with the results of Toma & Murphy (1977) on nuggets from Colombia. The concentration of Rh and Pd attains 2.4 and 3.4 wt.%, respectively, and Os, up to 2.2 wt.%. One composition (#69) shows an unusually high content of Ir, 11 wt.%. The Fe content of the grains of alloy varies between 15 and 27 at.%. A frequency distribution (Fig. 4) shows that 82% of the analyzed grains have an Fe content between 15 and 21 at.%, with a peak at 18 at.%. Using the nomenclature of Cabri & Feather (1975), these grains would mainly correspond to "native platinum", and a few of them, to "ferroan platinum". Only 18% of the grains have an Fe content between 23 and 27 at.%, which could correspond to "isoferroplatinum". These results confirm the observations of Johan *et al.* (1990),

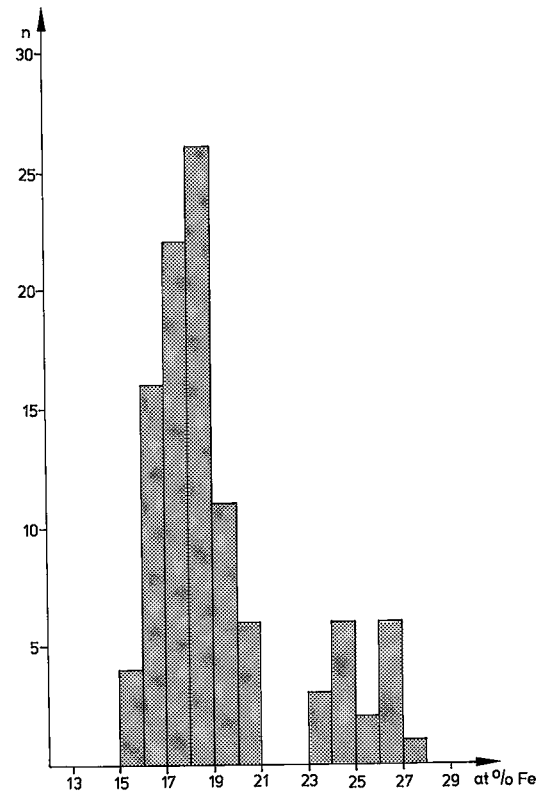


FIG. 4. Frequency distribution of Fe (at.%) in Pt–Fe alloys.

TABLE 2. CHEMICAL COMPOSITION* OF Ru-Os-Ir-Pt ALLOY

| | weight per cent | | | |
|---|---|---|---|---|
| Analysis No. | 104 | 114 | 143 | 145 |
| Ru | 1.19 | 1.14 | 4.57 | 2.09 |
| Rh | 0.61 | 0.88 | 2.76 | 2.85 |
| Pd | – | – | 0.43 | – |
| Os | 92.71 | 70.91 | 73.55 | 68.52 |
| Ir | 1.85 | 15.36 | 11.90 | 14.89 |
| Pt | 1.14 | 8.91 | 5.92 | 11.03 |
| Fe | – | 0.29 | – | 0.24 |
| Cu | – | 0.21 | – | 0.33 |
| Total | 97.50 | 97.70 | 99.13 | 99.95 |
| | atomic proportions | | | |
| Ru | 0.023 | 0.021 | 0.082 | 0.037 |
| Rh | 0.011 | 0.016 | 0.048 | 0.050 |
| Pd | – | – | 0.007 | – |
| Os | 0.936 | 0.708 | 0.697 | 0.652 |
| Ir | 0.018 | 0.152 | 0.112 | 0.140 |
| Pt | 0.011 | 0.087 | 0.055 | 0.102 |
| Fe | – | 0.010 | – | 0.008 |
| Cu | – | 0.006 | – | 0.009 |

* Obtained by electron-microprobe analysis. All other elements were found to be below their limits of detection.

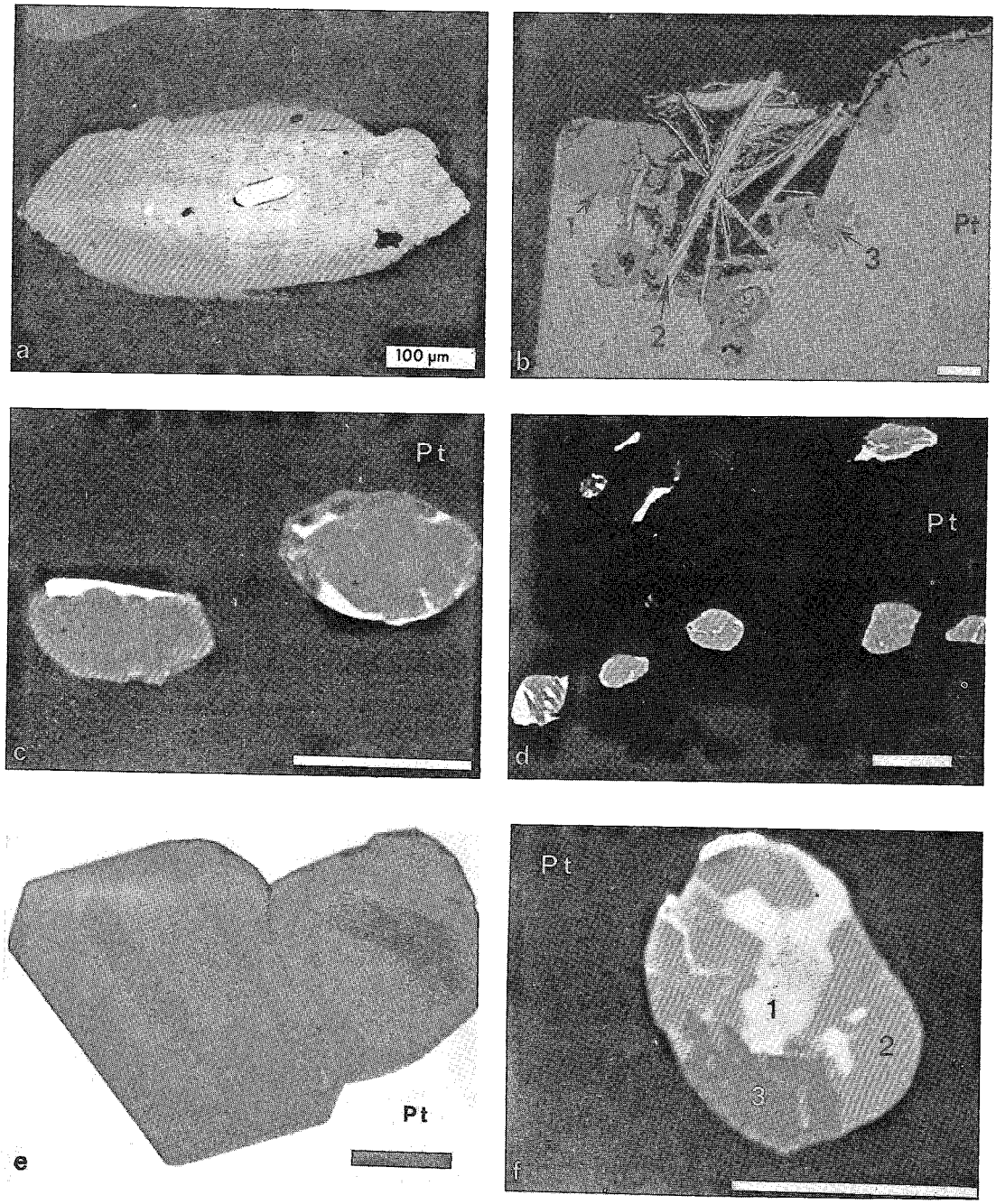


FIG. 5. Back-scattered electron images (BEI) of various PGM. a. Pt–Fe alloy with inclusion of osmium. b. Pt–Fe alloy with a rim of an unknown Pt–Cu–S phase (1), lamella of Pt-rich osmium (2) and an inclusion of hongshiite (3). c. Inclusions of bowieite in Pt–Fe alloy. d. Crystallographically oriented inclusions of cuprorhodsite in Pt–Fe alloy. e. Zoned crystals of laurite enclosed in Pt–Fe alloy. f. Intergrowth of bowieite (1), braggite (2), and an unknown Pd–As–Te phase (3) as inclusion in Pt–Fe alloy. Scale bar represents 10 μm (except Fig. 5a).

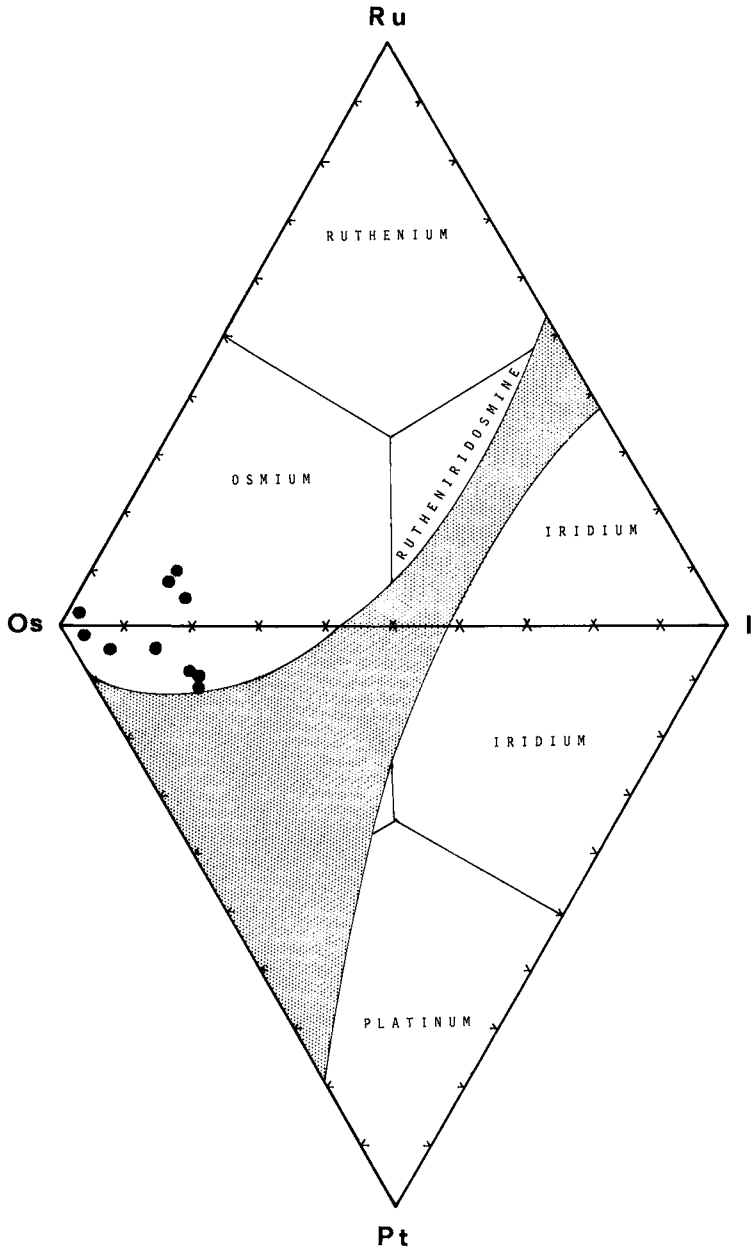


FIG. 6. Plot of compositions (electron-microprobe data) of natural alloy in the system Ru–Os–Ir–Pt (small amounts of Rh, Pd, Fe and Cu are not considered in the plot); nomenclature and miscibility gap modified after Harris & Cabri (1991).

but are contrary to their findings in the lack of compositions with an Fe content between 21 and 23 at.%.

Inclusions of other minerals occur in less than 20% of the grains examined. In some cases, the inclusions show a specific crystallographic orientation within the Pt–Fe alloy. In contrast to the results of Johan *et al.* (1990), the inclusions are mainly found in "native platinum"; there are only a few exceptions.

*Pt–Cu alloy*

Hongshiite was found as a euhedral inclusion 20 μm across in Pt–Fe alloy (Fig. 5b). Compared with the host mineral, it is a little darker, with a brownish tinge under the microscope in air. The composition (Table 1, #146) shows traces of Os and Ir, but no Ru, Rh, Pd, Fe and Ni.

*Ru–Os–Ir alloy*

Grains of a Ru–Os–Ir alloy occur as small "droplets" or as lamellae up to 75 μm long in Pt–Fe alloy (Fig. 5a). Under reflected light, these grains are white with a light blue tinge and always strongly anisotropic, which indicates that the alloy is not cubic. Results of electron-microprobe analyses (Table 2) confirm the microscopic observations concerning the crystal structure. They show a dominance of Os in all grains. The content of Os varies between 72.9 and 95.8 at.%, and Ir is invariably present, varying between 1.9 and 16.3 at.%. Compared to this, the Ru content is consistently very low (0 – 9.2 at.%). Pt is present in some grains (up to 11.4 at.%). All analyses show small amounts of Rh (0.6 – 2.9 wt.%). Using the revised nomenclature of Harris & Cabri (1991), all compositions fall in the field of osmium (Fig. 6). One 40-μm-long lamella near the margin of a grain of Pt–Fe alloy (Fig. 5b) contains 11.4 at.% Pt (Table 2, #145). It lies in the miscibility gap proposed by Harris & Cabri (1991). The original boundaries of the miscibility gap were drawn on the basis of the few available analytical data; in Figure 6, they have been adjusted to include our new data.

The Ru–Os–Ir alloy from the Santiago River differs considerably in its composition from that found at some other localities, *e.g.*, Papua New Guinea (Harris & Cabri 1973), Kamchatka (Razin *et al.* 1979), Tasmania (Ford 1981), Mongolia (Sidorov *et al.* 1987) or Burma (Hagen *et al.* 1990) where the alloys contain much more Ru. However, it is similar to alloys reported from Tulameen and Spruce Creek, British Columbia, by Harris & Cabri (1973) and to most compositions from the Durance River, France (Johan *et al.* 1990).

*Bowieite*

The most common sulfide mineral in the sample is bowieite. It occurs as euhedral to subhedral inclusions up to 50 μm across, both as discrete grains (Fig. 5c) or intergrown with cooperite. Microprobe analyses (Table 3) show a mean composition of 59.5 wt.% Rh, 3.8 wt.% Pt and 31.4 wt.% S, and only traces of Ru and Ir and, locally, Pd. This corresponds to the general formula $(Rh_{1.82}Pt_{0.06}Ir_{0.03})_{\Sigma=1.91}S_{3.09}$ and is very close to the ideal formula $Rh_2S_3$. Compared with the original description of bowieite from Goodnews Bay, Alaska, by Desborough & Criddle (1984), the very low content of Ir is noteworthy. This can be explained by the low Ir content throughout the whole assemblage of PGM from the Santiago River.

TABLE 3. CHEMICAL COMPOSITION* OF BOWIEITE

| | weight per cent | | |
|---|---|---|---|
| Analysis No. | 117 | 130 | 134 |
| Ru | 1.46 | 0.33 | 1.25 |
| Rh | 54.50 | 59.04 | 59.85 |
| Os | 0.16 | 0.10 | 0.20 |
| Ir | 3.16 | 2.94 | 2.99 |
| Pt | 7.09 | 2.95 | 4.12 |
| Fe | 0.36 | 0.15 | 0.25 |
| S | 31.17 | 31.38 | 29.68 |
| Total | 97.90 | 96.89 | 98.34 |
| | atomic proportions | | |
| Ru | 0.046 | 0.010 | 0.040 |
| Rh | 1.680 | 1.805 | 1.862 |
| Os | 0.003 | 0.002 | 0.003 |
| Ir | 0.052 | 0.048 | 0.050 |
| Pt | 0.115 | 0.048 | 0.068 |
| Fe | 0.021 | 0.009 | 0.014 |
| S | 3.083 | 3.079 | 2.963 |

* Obtained by electron-microprobe analysis. All other elements were found to be below their limits of detection.

*Cuprorhodsite*

Cuprorhodsite is nearly as common as bowieite. The euhedral or subhedral grains up to 25 μm across normally occur as isolated crystallographically oriented inclusions in Pt–Fe alloy (Fig. 5d), intergrown with braggite in one case, and once together with bowieite in the same host mineral. Microprobe analyses show a large variation in composition, between 45.9 and 77.5 mol % cuprorhodsite (Table 4, Fig. 7). The compositions define two different groups. One group has a cuproiridsite

TABLE 4. CHEMICAL COMPOSITION* OF CUPRORHODSITE

| | weight per cent | | | |
|---|---|---|---|---|
| Analysis No. | 107 | 110 | 113 | 160 |
| Ru | 0.87 | 0.57 | 0.28 | – |
| Rh | 33.76 | 27.21 | 18.36 | 29.70 |
| Pd | – | 5.58 | – | – |
| Os | 0.47 | 0.94 | 0.28 | 0.28 |
| Ir | 0.74 | 0.37 | 13.88 | 16.91 |
| Pt | 17.70 | 23.04 | 27.14 | 12.03 |
| Fe | 4.15 | 6.19 | 0.99 | 2.16 |
| Cu | 10.43 | 10.44 | 11.17 | 10.79 |
| Ni | 0.54 | 0.73 | – | – |
| S | 30.93 | 24.62 | 25.86 | 28.99 |
| Total | 99.58 | 99.69 | 97.96 | 100.86 |
| | atomic proportions | | | |
| Ru | 0.036 | 0.027 | 0.014 | – |
| Rh | 1.395 | 1.231 | 0.896 | 1.301 |
| Pd | – | 0.244 | – | – |
| Os | 0.010 | 0.023 | 0.007 | 0.007 |
| Ir | 0.016 | 0.009 | 0.363 | 0.397 |
| Pt | 0.386 | 0.550 | 0.698 | 0.278 |
| Fe | 0.316 | 0.516 | 0.089 | 0.175 |
| Cu | 0.698 | 0.766 | 0.883 | 0.765 |
| Ni | 0.039 | 0.058 | – | – |
| S | 4.103 | 3.576 | 4.050 | 4.077 |

* Obtained by electron-microprobe analysis. All other elements were found to be below their limits of detection.

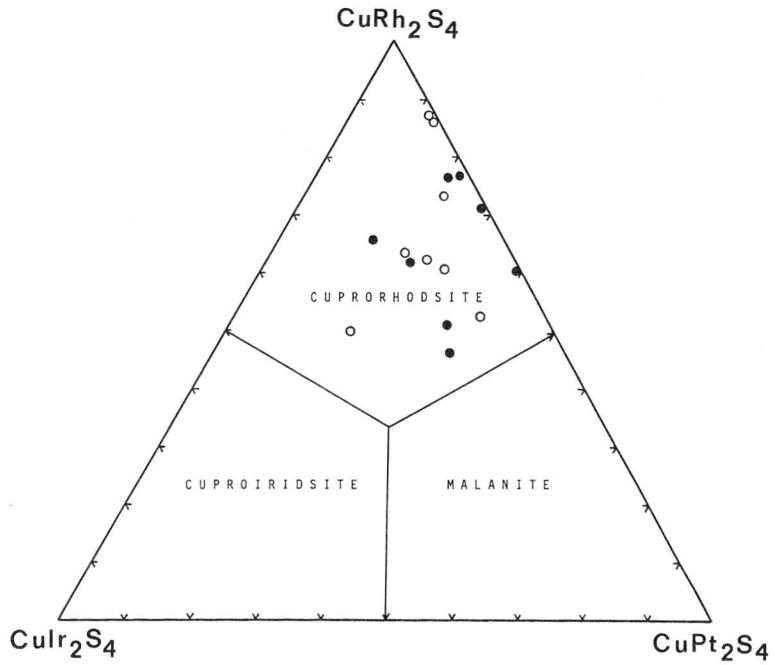


FIG. 7. Plot of compositions (electron-microprobe data) of cuprorhodsite. Solid circles: Santiago River, Esmeraldas Province, Ecuador; open circles: Durance River, France (after Johan *et al.* 1990).

content of 16 to 20 mol %, and varies in malanite content between 14 and 36 mol %. The other group has less than 3 mol % cuproiridsite and 20 to 39 mol % malanite. In all grains, part of the Cu is replaced by iron (up to 6.2 wt.%), but nickel occurs in trace amounts only. The high Pd content, in some cases up to 5.6 wt.% (Table 4, #110), is striking. In one case (Table 4, #107), the calculation of the formula shows a surplus in sulfur, and in another (Table 4, #110), a deficiency. Both the chemical composition of the cuprorhodsite and the fact that there are distinctly different groups, as shown in Figure 7, match the results of Johan *et al.* (1990).

*Laurite–Erlichmanite*

These minerals are not very common in the samples from the Santiago River. They form single euhedral to subhedral grains up to 75 μm across. The analytical results (Table 5, Fig. 8) show that the Ru content varies between 51 and 81 mol %. The Ir content is usually very low (0.6 – 2.5 mol % $IrS_2$), with the exception of one crystal of erlichmanite that contains 8.1 mol % $IrS_2$ (Table 5, #123). Another grain of erlichmanite contains up to 3.8 wt.% Rh (Table 5, #159).

One inclusion comprising two intergrown euhedral crystals of laurite (30 × 40 μm) in Pt–Fe alloy looks homogeneous under the microscope, but the back-scattered electron image (BEI) displays unusual zoning (Fig. 5e). Electron-microprobe analyses show that the lamella in the center of the larger crystal is the most Os-rich part of the intergrowth and contains 46.4 mol % $OsS_2$ (Table 5, #154). The lamella is surrounded by a region enriched in Ru, *i.e.*, 76.0 mol % $RuS_2$ (Table 5, #152). Some drop-like areas in the crystal and the margin have a composition between these values (Table 5, #153, 156, 157). The Ir content is consistently low (less than 2.5

TABLE 5. CHEMICAL COMPOSITION* OF LAURITE/ERLICHMANITE

| | | | weight per cent | | | | | |
|---|---|---|---|---|---|---|---|---|
| Anal | 116 | 123 | 152 | 153 | 154 | 156 | 157 | 159 |
| Ru | 40.34 | 17.77 | 37.37 | 30.55 | 19.96 | 33.77 | 24.74 | 17.95 |
| Rh | 1.82 | 0.38 | 2.26 | 2.85 | 3.30 | 2.40 | 3.03 | 3.78 |
| Pd | - | - | - | - | - | 0.15 | - | - |
| Os | 15.94 | 42.95 | 22.30 | 30.25 | 39.85 | 27.19 | 35.94 | 43.48 |
| Ir | 2.14 | 6.84 | 1.20 | 1.41 | 2.18 | 0.63 | 1.31 | 0.77 |
| Pt | 1.88 | 0.67 | 0.61 | 0.94 | 0.79 | 0.98 | 0.95 | 2.70 |
| S | 35.31 | 29.94 | 35.33 | 33.07 | 31.71 | 33.91 | 31.96 | 30.73 |
| Total | 97.43 | 98.55 | 99.07 | 99.07 | 97.78 | 99.03 | 97.93 | 99.41 |
| | | | atomic proportions | | | | | |
| Ru | 0.738 | 0.383 | 0.685 | 0.592 | 0.410 | 0.639 | 0.500 | 0.375 |
| Rh | 0.033 | 0.008 | 0.041 | 0.054 | 0.067 | 0.045 | 0.060 | 0.078 |
| Pd | - | - | - | - | - | 0.003 | - | - |
| Os | 0.155 | 0.492 | 0.217 | 0.311 | 0.436 | 0.274 | 0.385 | 0.483 |
| Ir | 0.021 | 0.077 | 0.012 | 0.014 | 0.024 | 0.006 | 0.014 | 0.008 |
| Pt | 0.018 | 0.007 | 0.006 | 0.009 | 0.008 | 0.010 | 0.010 | 0.029 |
| S | 2.036 | 2.033 | 2.039 | 2.018 | 2.055 | 2.024 | 2.031 | 2.026 |

* Obtained by electron-microprobe analysis. All other elements were found to be below their limits of detection.

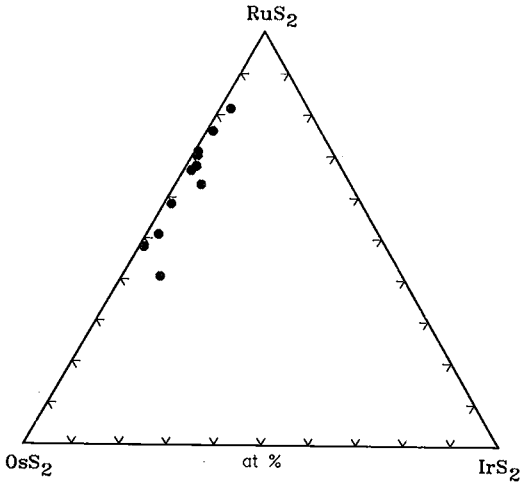


FIG. 8. Plot of compositions of PGM (electron-microprobe data) in terms of the system $RuS_2$–$OsS_2$–$IrS_2$.

mol % $IrS_2$). All parts of the crystal have a nearly constant amount of Rh, 2.5 to 3.0 wt.%. The intergrowth of different Os- and Ru-rich phases can be explained by variation of the Os/Ru ratio in the adjacent melt during primary crystallization.

*Cooperite*

Cooperite mostly forms euhedral crystals up to 25 μm across, intergrown with bowieite. In one case, it forms a rim around Pt–Fe alloy and is partly replaced by sperrylite. The electron-microprobe analyses (Table 6) show that the PtS content ranges between 72.4 and 98.1 mol %. NiS is invariably very low (0.9 – 3.4 mol %). One grain contains 2.6 wt.% Rh (Table 6, #131).

TABLE 6. CHEMICAL COMPOSITION* OF COOPERITE/BRAGGITE

| | weight per cent | | | |
|---|---|---|---|---|
| Analysis No. | 118 | 131 | 138 | 148 |
| Ru | - | 0.50 | 0.05 | - |
| Rh | 1.44 | 2.55 | 0.09 | 0.24 |
| Pd | 12.59 | 6.04 | 0.47 | 47.96 |
| Os | 0.23 | 0.30 | 0.35 | 0.10 |
| Ir | 0.45 | 0.16 | 0.44 | 0.11 |
| Pt | 69.26 | 75.06 | 83.48 | 29.76 |
| Fe | 0.51 | 0.49 | 0.15 | 0.13 |
| Cu | 0.16 | 0.23 | 0.09 | 0.23 |
| Ni | 0.33 | 0.20 | - | 1.30 |
| S | 16.63 | 15.95 | 14.98 | 21.23 |
| As | - | 0.19 | - | - |
| Total | 101.60 | 101.67 | 101.10 | 101.06 |
| | atomic proportions | | | |
| Ru | - | 0.010 | 0.001 | - |
| Rh | 0.027 | 0.050 | 0.002 | 0.004 |
| Pd | 0.230 | 0.115 | 0.010 | 0.695 |
| Os | 0.002 | 0.003 | 0.004 | 0.001 |
| Ir | 0.005 | 0.002 | 0.005 | 0.001 |
| Pt | 0.691 | 0.778 | 0.941 | 0.235 |
| Fe | 0.018 | 0.018 | 0.006 | 0.004 |
| Cu | 0.005 | 0.007 | 0.003 | 0.006 |
| Ni | 0.011 | 0.007 | - | 0.034 |
| S | 1.011 | 1.006 | 1.028 | 1.022 |
| As | - | 0.005 | - | - |

* Obtained by electron-microprobe analysis. All other elements were found to be below their limits of detection.

*Braggite*

Braggite is very rare; it occurs as small xenomorphic grains (<15 μm) intergrown with cuprorhodsite or bowieite. The general formula corresponds to $(Pd_{0.70}Pt_{0.24}Ni_{0.03}Cu_{0.01})_{\Sigma=0.98}S_{1.02}$ (Table 6, #148).

*Sperrylite*

This mineral only occurs as a thin rim replacing the cooperite that coats Pt–Fe alloy. It contains 1.8 wt.% Rh, whereas the cooperite is free of Rh and contains 3.5 wt.% S substituting for As.

*Unnamed palladium phases*

Two different palladium-rich phases occur as inclusions in grains of Pt–Fe alloy; they are always intergrown with bowieite. Owing to the small size of the grains (<10 μm), the optical properties could not be determined precisely. One drop-like grain, intergrown with bowieite and braggite (Fig. 5f), shows a brownish color with a light yellow tinge and seems to be slightly anisotropic in air. The composition (Table 7, #129) corresponds to that of a Pd–As–Te phase devoid of Sb. The formula was calculated as $(Pd_{2.84}Pt_{0.04}Cu_{0.04})_{\Sigma=2.92}(As_{0.50}Te_{0.46}S_{0.11})_{\Sigma=1.07}$ or, if the small amounts of Pt, Cu and S are put down to analytical contamination, as $Pd_{2.99}(As_{0.52}Te_{0.49})_{\Sigma=1.01}$. This is an intermediate phase between guanglinite $Pd_3As$ and keithconnite $Pd_{3-x}Te$, and more closely corresponds in composition to the phase $Pd_{2.6}As_{0.53}(Te_{0.42}Bi_{0.05})_{\Sigma=0.47}$, reported by Kovalenker *et al.* (1973), than to vincentite $(Pd,Pt)_3(As,Sb,Te)$, reported by Stumpfl & Tarkian (1974). It can only be said at the moment that this is an unknown palladium phase; this is in line with the critical remarks by Cabri (1980) on the original description of vincentite.

Another small grain that appears yellowish and is isotropic in air under the ore microscope is a palladium–copper sulfide with a noticeable amount of Rh (Table 7, #108). Its formula was calculated as $(Pd_{2.52}Rh_{0.18}Pt_{0.13}Ru_{0.03})_{\Sigma=2.86}(Cu_{0.93}Fe_{0.17})_{\Sigma=1.10}S_{2.03}$. This is close to the phase $(Cu,Fe)_{1-x}(Pd,Rh,Pt)_{2+x}S_2$ described by Johan *et al.* (1990).

*Unnamed Pt–Cu sulfide*

Some grains of Pt–Fe alloy have a narrow rim (Fig. 5b) which, under reflected light in air, looks fine-grained and inhomogeneous, with a light blue color and some internal reflections. Results of two electron-microprobe analyses of the rim show the dominance of Pt, Cu and S

TABLE 7. CHEMICAL COMPOSITION* OF UNKNOWN PGE PHASE

| | weight per cent | | | |
|---|---|---|---|---|
| Analysis No. | 108 | 129 | 142 | 147 |
| Ru | 0.58 | - | 5.15 | 3.56 |
| Rh | 3.92 | - | 2.54 | 2.45 |
| Pd | 57.72 | 74.61 | - | - |
| Os | 0.21 | 0.11 | 3.02 | 1.97 |
| Ir | - | - | 2.73 | 2.09 |
| Pt | 5.26 | 2.02 | 60.90 | 63.78 |
| Fe | 2.05 | - | - | - |
| Cu | 12.65 | 0.64 | 18.27 | 19.66 |
| Ni | 0.27 | - | - | - |
| S | 14.05 | 0.90 | 5.18 | 3.46 |
| Te | - | 14.57 | - | - |
| As | - | 9.17 | 1.17 | 1.93 |
| Total | 96.71 | 102.02 | 98.96 | 98.90 |
| | atomic proportions | | | |
| Ru | 0.026 | - | 1.443 | 1.076 |
| Rh | 0.177 | - | 0.700 | 0.728 |
| Pd | 2.517 | 2.842 | - | - |
| Os | 0.005 | 0.002 | 0.449 | 0.317 |
| Ir | - | - | 0.402 | 0.332 |
| Pt | 0.125 | 0.042 | 8.842 | 9.997 |
| Fe | 0.171 | - | - | - |
| Cu | 0.924 | 0.041 | 9.146 | 9.461 |
| Ni | 0.021 | - | - | - |
| S | 2.033 | 0.114 | 4.572 | 3.300 |
| Te | - | 0.463 | - | - |
| As | - | 0.496 | 0.444 | 0.788 |

* Obtained by electron-microprobe analysis. All other elements were found to be below their limits of detection.

(Table 7, #142, 147). The elements Ru, Rh, Os, Ir, and As also are present in small amounts. The calculated formulae range between $Pt_{12}Cu_8S_5$ and $Pt_{12}Cu_{10}S_4$. This confirms the observed inhomogeneity of this material of obviously secondary origin. It does not correspond to any known mineral in the Pt–Cu–S system and can only be reported as a possible new phase.

*Chalcopyrite*

Chalcopyrite is the only base-metal sulfide found as an inclusion in Pt–Fe alloy. The grain is 15 μm across and intergrown with cuprorhodsite.

## Discussion and Conclusions

The concentrate of PGM that we investigated from the Santiago River is surprisingly monotonous in its mineral composition compared with other PGM placers, *e.g.*, from British Columbia (Raicevic & Cabri 1976, Nixon *et al.* 1990), Burma (Hagen *et al.* 1990), Finland (Törnroos & Vuorelainen 1987), France (Johan *et al.* 1990), Kamchatka (Razin *et al.* 1979), Papua New Guinea (Harris 1974) or Tasmania (Ford 1981). It exclusively contains Pt–Fe alloy as individual grains, whereas all other observed grains of alloy and sulfides of the platinum-group elements only occur as inclusions in Pt–Fe alloy or, rarely, as a rim on grains of Pt–Fe alloy. The grains are mostly well rounded by abrasion during transport.

The droplet shape of osmium inclusions suggests that they were trapped in a liquid state. The mostly euhedral shape and the crystallographic orientation of cuprorhodsite in the host mineral indicate primary formation from a complex Pt–Rh–Ir–Fe–Cu–S solid solution. A similar origin is inferred for the euhedral inclusions of hongshiite, bowieite, laurite and cooperite. The rarely observed rims of cooperite, sperrylite and the unknown Pt–Cu sulfides on Pt–Fe alloys are obviously secondary products.

The Pt–Fe alloys and especially the inclusions of Ru–Os–Ir alloy are characterized by a very low content of ruthenium, and ruthenium minerals are very rare. On the other hand, the Pt–Fe alloys always contain remarkable amounts of Rh, and the rhodium sulfides bowieite and cuprorhodsite are the most common inclusions. All other PGM also contain a significant amount of Rh. These features indicate a Ru-depleted and Rh-enriched source for the PGM from the Santiago River. A similar trend was found by the first author in PGM placers from the Condoto River area, Chocó Department, Colombia (unpubl. data).

A depletion of Ru and enrichment of Rh in alloys together with the occurrence of Rh sulfide have been reported from PGE mineralization associated with mafic–ultramafic Alaskan-type intrusions from Kamchatka (Zhdanov & Rudashevskii 1980, Rudashevskii & Zhdanov 1983) and Australia (Johan *et al.* 1989). Moreover, all placer deposits derived from Alaskan-type intrusions, *e.g.*, at Goodnews Bay, Alaska (Mertie 1976), Tulameen, British Columbia (Raicevic & Cabri 1976, Nixon *et al.* 1990), Nizhnii Tagil, Ural and Aldan shield, Siberia (Razin 1976) and New South Wales, Australia (Slansky *et al.* 1991) show a significant dominance of Pt–Fe alloy.

The basic to ultrabasic rocks that occur in the Macuchi Formation have been interpreted as part of an ophiolite complex and, therefore, have been considered to be the possible source-rock for the PGM placers in the rivers west of the Cordillera de Toisán. The mineralogical and chemical compositions of the PGM from the Santiago River compare closely with those of PGM placers from Burma (Hagen *et al.* 1990), which undoubtedly derive from ophiolites, and those from Alaskan-type intrusions in Alaska (Mertie 1976) and British Columbia (Raicevic & Cabri 1976, Nixon *et al.* 1990). If the results of Zhdanov & Rudashevskii (1980), Rudashevskii & Zhdanov (1983) and Johan *et al.* (1989) can be accepted as a general rule, then the PGM in the placers of the Santiago River, Esmeraldas Province, Ecuador, could well originate from a mafic–ultramafic Alaskan-type intrusion whose exact nature and location are still unknown.

## Acknowledgements

The authors thank INEMIN for access to unpublished technical reports. They are indebted to Mr. C.E.

Knowles, Jr., manager of the Compañia Minera Gowanda S.A., who kindly provided several grains of platinum-group minerals from the Santiago River area. We also thank the following colleagues of the Federal Institute for Geosciences and Natural Resources: Dr. P. Müller for performing the mineral separation and for helpful discussions, E. Knickrehm for the SEM photomicrographs, and J. Lodziak II for carrying out the electron-microprobe analyses. We are also grateful to Drs. L.J. Cabri, R.F. Martin, G.T. Nixon and an anonymous referee for helpful comments.

## REFERENCES

BALDOCK, J.W. (1982): Geology of Ecuador. *Expl. Bull., Nat. Geol. Map of the Rep. of Ecuador, 1:1 Mio, Quito – London.*

_____ (1985): The northern Andes: a review of the Ecuadorian Pacific margin. *In* The Ocean Basins and Margins **7A** (A.E.M. Nairn, F.G. Stehli & S. Uyeda, eds.). Plenum Press, New York (181-217).

CABRI, L.J. (1980): Determination of ideal formula for new minerals of the platinum-group. *Proc. Int. Mineral. Assoc. (XIth, Novosibirsk)* **1**, *Academy of Science, Moscow* (157-165).

_____ & FEATHER, C.E. (1975): Platinum-iron alloys: a nomenclature based on a study of natural and synthetic alloys. *Can. Mineral.* **13**, 117-126.

DESBOROUGH, G.A. & CRIDDLE, A.J. (1984): Bowieite: a new rhodium–iridium platinum sulfide in platinum-alloy nuggets, Goodnews Bay, Alaska. *Can. Mineral.* **22**, 543-552.

EVANS, C.D.R. & WHITTAKER, J.F. (1982): The geology of the western part of the Borbón Basin, north-west Ecuador. *In* Trench–Forearc Geology: Sedimentation and Tectonics on Modern and Ancient Active Plate Margins (J.K. Leggett, ed.). Blackwell, Oxford (191-198).

FORD, R.J. (1981): Platinum-group minerals in Tasmania. *Econ. Geol.* **76**, 498-504.

HAGEN, D., WEISER, T. & THAN HTAY (1990): Platinum-group minerals in Quaternary gold placers in the Upper Chindwin area of northern Burma. *Mineral. Petrol.* **42**, 265-286.

HARRIS, D.C. (1974): Ruthenarsenite and iridarsenite, two new minerals from the territory of Papua and New Guinea and associated irarsite, laurite and cubic iron-bearing platinum. *Can. Mineral.* **12**, 280-284.

_____ & CABRI, L.J. (1973): The nomenclature of the natural alloys of osmium, iridium and ruthenium based on new compositional data of alloys from world-wide occurrences. *Can. Mineral.* **12**, 104-112.

_____ & _____ (1991): Nomenclature of platinum-group-element alloys: review and revision. *Can. Mineral.* **29**, 231-237.

HENDERSON, W.G. (1981): The volcanic Macuchi Formation, Andes of northern Ecuador. *Newslett. Stratigraphy* **9**, 157-168.

JOHAN, Z., OHNENSTETTER, M., FISCHER, W. & AMOSSÉ, J. (1990): Platinum-group minerals from the Durance River alluvium, France. *Mineral. Petrol.* **42**, 287-306.

_____, _____, SLANSKY, E., BARRON, L.M. & SUPPEL, D. (1989): Platinum mineralization in the Alaskan-type intrusive complex near Fifield, New South Wales, Australia. 1. Platinum-group minerals in clinopyroxenites of the Kelvin Grove prospect, Owendale Intrusion. *Mineral. Petrol.* **40**, 289-309.

KENNERLY, J.B. (1980): Outline of the geology of Ecuador. *Overseas Geol. Mineral. Res.* **55**, 1-17.

KOVALENKER, V.A., LAPUTINA, I.P., VYAL'SOV, L.N., GENKIN, A.D. & YEVSTIGNEYEVA, T.L. (1973): Tellurium minerals in copper–nickel sulfide ores at Talnakh and Oktyabr' (Noril'sk district). *Int. Geol. Rev.* **15**, 1284-1294.

MERTIE, J.B., JR. (1976): Platinum deposits of the Goodnews Bay district, Alaska. *U.S. Geol. Surv., Prof. Pap.* **938**.

NIXON, G.T., CABRI, L.J. & LAFLAMME, J.H.G. (1990): Platinum-group-element mineralization in lode and placer deposits associated with the Tulameen Alaskan-type complex, British Columbia. *Can. Mineral.* **28**, 503-535.

PALADINES, P.A. & SANMARTIN, D.M. (1980): Mapa Metalogénico del Ecuador, 1:1 Mio. *Ministerio de Resursos Naturales y Energético, Quito, Ecuador.*

RAICEVIC, D. & CABRI, L.J. (1976): Mineralogy and concentration of Au- and Pt-bearing placers from the Tulameen River area in British Columbia. *Can. Inst. Min. Metall. Bull.* **69**(770), 111-119.

RAZIN, L.V. (1976): Geologic and genetic features of forsterite dunites and their platinum-group mineralization. *Econ. Geol.* **71**, 1371-1376.

_____, MOCHALOV, A.G., RAZINA, T.P. & CHUBAROV, V.M. (1979): Minerals of platinum metals in alluvial placers in an area of hyperbasite massifs (Koryak-Kamchatka region). *Geol. Geofiz.* **20**(12), 72-79 (in Russ.).

RUDASHEVSKII, N.S. & ZHDANOV, V.V. (1983): Accessory platinum mineralization within a mafic-ultramafic intrusion in Kamchatka. *Bull. Mosc. Obshchest. Izpyt Prirody otd. geol.* **58**, 49-59 (in Russ.).

SIDOROV, E.G., IZOKH, A.E., KRIVENKO, A.P. & CHUBAROV, V.M. (1987): Platinum minerals of Siberia. *Geol. Geofiz.* **28**(12), 101-104 (in Russ.).

SLANSKY, E., JOHAN, Z., OHNENSTETTER, M., BARRON, L.M. & SUPPEL, D. (1991): Platinum mineralization in the Alaskan-type intrusive complex near Fifield, N.S.W., Australia. 2. Platinum-group minerals in placer deposits at Fifield. *Mineral. Petrol.* **43**, 161-180.

STUMPFL, E.F. & TARKIAN, M. (1974): Vincentite, a new

palladium mineral from southeast Borneo. *Mineral. Mag.* **39**, 525-527.

TOMA, S.A. & MURPHY, S. (1977): The composition and properties of some native platinum concentrates from different localities. *Can. Mineral.* **15**, 59-69.

TÖRNROOS, R. & VUORELAINEN, Y. (1987): Platinum-group metals and their alloys in nuggets from alluvial deposits in Finnish Lapland. *Lithos* **20**, 491-500.

ZHDANOV, V.V. & RUDASHEVSKII, N.S. (1980): New type of Au–Pt mineralization in metasomatites on basites. *Dokl. Akad. Nauk SSSR* **252**, 1452-1456 (in Russ.).

*Received August 21, 1991, revised manuscript accepted July 1, 1992.*